

A 3D Polar Nanotubular Coordination Polymer with Dynamic Structural Transformation and Ferroelectric and Nonlinear-Optical Properties

Lina Li,^{†,‡} Jingxin Ma,[†] Cheng Song,^{||} Tianliang Chen,^{†,‡} Zhihua Sun,[†] Shuyun Wang,^{†,‡} Junhua Luo,^{*,†} and Maochun Hong[†]

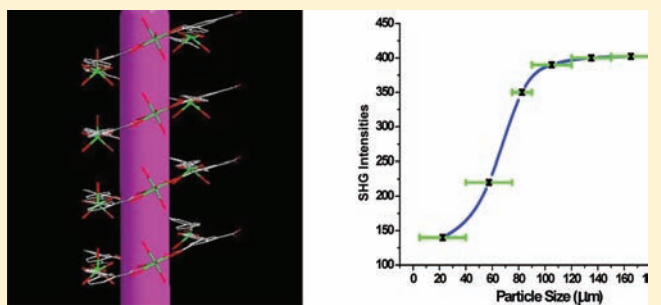
[†]Key Laboratory of Optoelectronic Materials Chemistry and Physics, Fujian Institute of Research on the Structure of Matter, Chinese Academy of Sciences, Fuzhou 350002, China

[‡]Graduate School of the Chinese Academy of Sciences, Beijing 100039, China

^{||}Department of Chemistry, Jiangxi Normal University, Nanchang 330022, P.R. China

Supporting Information

ABSTRACT: A chiral coordination nanotube, $[\text{Cd}_3(\text{BPT})_2(\text{H}_2\text{O})_9] \cdot 2\text{H}_2\text{O}$ (Cd-1; BPT = biphenyl-3,4',5-tricarboxylate), has been synthesized from achiral components and structurally characterized. It consists of homochiral channels based on right-handed helical chains and shows an interdigitated interaction to give a chiral 3D network. The chiral nanotubular framework exhibits dynamic structural transformation upon removal of the guest molecules, and the polarity of this compound induces it to display both ferroelectric and nonlinear-optical properties.



INTRODUCTION

Nanotubular materials have attracted considerable interest as a result of their novel structures¹ and potential applications in nanoelectronics, molecular devices and sensors, and ion exchange.² Furthermore, chiral nanotubes have stimulated extensive research owing to their intriguing architectures³ and applications in enantioselective separation and asymmetric catalysts.⁴ Up to now, some chiral coordination nanotubes with intriguing structures and properties have been reported. An interlocked metal–organic chiral nanotube built from C_2 -symmetric bipyridyl ligands and linear metal-connecting points has been reported by Lin's group, who played an important role in the research of chiral coordination nanotubular networks.⁵ Huang and co-workers recently reported a chiral nanotubular polymer exhibiting single-crystal–single-crystal oxidation transformation formed by an array of single-stranded helices.⁶ Cui's group has synthesized several homochiral nanotubular frameworks based on enantiopure ligands.⁷ On the other hand, chirality can induce novel functions such as nonlinear-optical (NLO)⁸ and ferroelectric properties,⁹ resulting in multifunctional molecular materials.

Nonlinear second harmonic generation (SHG) and ferroelectric materials are very useful in a variety of areas such as electrooptical devices, light modulators, and information storage.¹⁰ Traditionally, research of ferroelectric materials has been mainly focused on inorganic compounds such as KH_2PO_4 (KDP), BaTiO_3 , and LiNbO_3 .¹¹ The development of ferroelectric materials based on metal–organic frameworks remains in its infancy.¹² In addition, second-order NLO materials have

also undergone transition from pure inorganic oxides to metal–organic coordination compounds, which combine the advantages of the inorganic metal ions and organic ligands. As far as we know, some porous metal–organic frameworks have been reported to exhibit both ferroelectric and NLO properties.¹³ However, it is still a challenge to synthesize new coordination materials with both ferroelectric and second-order NLO properties because such compounds must crystallize in acentric space groups belonging to the 10 polar point groups. Here we reported a polar compound, $[\text{Cd}_3(\text{BPT})_2(\text{H}_2\text{O})_9] \cdot 2\text{H}_2\text{O}$ (Cd-1; BPT = biphenyl-3,4',5-tricarboxylate), based on a long bridging ligand, biphenyl-3,4',5-tricarboxylic acid (H_3BPT),¹⁴ which is an intriguing 3D polar nanotubular coordination polymer based on helical chains, to display both ferroelectric properties and SHG response.

EXPERIMENTAL SECTION

Materials and Methods. The chemicals were purchased from commercial suppliers and used without further purification. Elemental analyses were determined on a Vario EL III elemental analyzer. The Fourier transform infrared (FT-IR) spectra were measured as KBr pellets on a Nicolet Magna 750 FT-IR spectrometer in the range of 4000–400 cm^{-1} . Thermogravimetric analyses (TGA) were performed on a Netzsch STA 449C thermal analyzer from room temperature to 800 °C under a nitrogen atmosphere at a heating rate of 10 °C min^{-1} . Powder X-ray diffraction (PXRD) patterns were collected in the 2θ range of 5–40° with a scan step of 0.05° in a sealed glass capillary on a

Received: November 8, 2011

Published: February 1, 2012

Rigaku MiniFlex diffractometer. The fluorescence measurements were performed on an Edinburgh Analytical FLS920 instrument. The UV absorption and optical diffuse-reflectance spectra were measured at room temperature with a PE Lambda 900 UV–visible spectrophotometer. The absorption spectrum was calculated from the reflectance spectrum using the Kubelka–Munk function:¹⁵ $\alpha/S = (1 - R)^2/(2R)$, where α is the absorption coefficient, S is the scattering coefficient, which is practically wavelength-independent when the particle size is larger than $5 \mu\text{m}$, and R is the reflectance. The NLO properties of $[\text{Cd}_3(\text{BPT})_2(\text{H}_2\text{O})_9] \cdot 2\text{H}_2\text{O}$ (**Cd-1**; BPT = biphenyl-3,4',5'-tricarboxylate) were tested on the sieved powder samples by the Kurtz and Perry method¹⁶ using an Nd:YAG laser (1064 nm) with an input pulse of 350 mV. The sample was ground and sieved into several distinct particle sizes. KDP powders of similar particle size were measured at the same time to serve as a reference.

Synthesis of Cd-1. $\text{Cd}(\text{NO}_3)_2 \cdot 4\text{H}_2\text{O}$ (0.06 mmol, 0.0185 g) and H_3BPT (0.04 mmol, 0.0114 g) were dissolved in a *N,N*-diethylformamide (DEF)/water (2 mL/1 mL) mixture. The solution was heated at 90 °C for 3 days to yield colorless plate crystals (yield: 43% based on Cd). Here DEF was not included in the product, but no crystals could be obtained without it, so it played a subtle role in dissolving the reactants and controlling the reaction. Anal. Calcd: C, 32.70; H, 3.29. Found: C, 32.62; H, 3.32. IR (KBr, cm^{-1}): 3392(m), 1615(m), 1546(vs), 1442(m), 1374(s), 1116(m), 864(m), 775(m), 734(m).

Single-Crystal Structure Determination. Single-crystal X-ray diffraction was performed on a Rigaku Mercury CCD diffractometer equipped with a fine-focus sealed-tube X-ray source (Mo $K\alpha$ radiation, graphite monochromator). *CrystalClear* software¹⁷ was used for data reduction and empirical absorption correction. The structure was solved by direct methods using *SHELXTL* and refined by full-matrix least squares on F^2 using *SHELX-97*.¹⁸ Non-hydrogen atoms were refined with anisotropic displacement parameters during the final cycles. Crystal data as well as details of the data collection and refinement for compounds are summarized in Table 1, and selected distance and angles are given in Table 2.

Table 1. Crystal Data and Structure Refinements for Cd-1

formula	$\text{Cd}_3\text{C}_{30}\text{O}_{23}\text{H}_{36}$
fw (g mol ⁻¹)	1101.82
cryst syst	monoclinic
space group	C_2
<i>a</i> (Å)	19.025(4)
<i>b</i> (Å)	7.339(12)
<i>c</i> (Å)	16.552(3)
<i>V</i> (Å ³)	2015.6(7)
<i>Z</i>	4
<i>T</i> (K)	293(2)
ρ_c (g cm ⁻³)	1.786
<i>F</i> (000)	1680.0
cryst size (mm ³)	0.5 × 0.45 × 0.1
data/restraints/param	3906/1/254
Flack parameter	0.01(4)
<i>R</i> 1, <i>wR</i> 2 ^a [<i>I</i> > 2 σ (<i>I</i>)]	0.0317, 0.1140
<i>R</i> 1, <i>wR</i> 2 (all data)	0.0321, 0.1156

$$^a R_1 = \frac{\sum ||F_o| - |F_c||}{\sum |F_o|}, \quad wR_2 = \left\{ \frac{\sum [w(F_o^2 - F_c^2)^2]}{\sum w(F_o^2)^2} \right\}^{1/2}$$

RESULTS AND DISCUSSION

Structure Description. **Cd-1** crystallizes in the chiral space group C_2 with a Flack parameter of 0.01(4), indicating enantiomeric purity of the single crystal of **Cd-1** despite the use of an achiral reagent. The asymmetric unit contains one and a half cadmium(II) centers, one bridging biphenyl-3,4',5-

Table 2. Selected Bond lengths [Å] and Angles [deg] for Cd-1

Cd(1)–O(8)	2.239(4)	Cd(2)–O(1)	2.275(5)
Cd(1)–O(7)	2.270(7)	Cd(2)–O(11)#2	2.312(5)
Cd(1)–O(6)#1	2.282(5)	Cd(2)–O(10)	2.327(4)
Cd(2)–O(5)	2.278(4)	Cd(2)–O(3)	2.565(4)
Cd(2)–O(12)	2.272(4)	Cd(2)–O(9)#2	2.569(4)
O(8)–Cd(1)–O(8) #1	171.5(3)	O(1)–Cd(2)–O(11) #2	89.9(2)
O(8)–Cd(1)–O(7)	85.73(14)	O(5)–Cd(2)–O(10)	95.93(19)
O(8)–Cd(1)–O(6) #1	79.77(18)	O(12)–Cd(2)–O(10)	83.91(17)
O(7)–Cd(1)–O(6) #1	134.06(17)	O(10)–Cd(2)–O(3)	96.93(15)
O(5)–Cd(2)–O(3)	53.03(14)	O(10)–Cd(2)–O(9) #2	90.21(15)
O(5)–Cd(2)– O(12)	138.86(17)	O(5)–Cd(2)–O(11) #2	84.40(15)
O(5)–Cd(2)–O(1)	89.1(2)	O(12)–Cd(2)–O(11) #2	136.37(16)
O(12)–Cd(2)– O(1)	95.1(2)		

^aSymmetry transformations used to generate equivalent atoms: #1, $-x + 2, y, -z + 3$; #2, $x - 1/2, y + 1/2, z$.

tricarboxylate group, four half-coordinated water molecules, and one guest water molecule. As shown in Figure 1, the Cd(1)

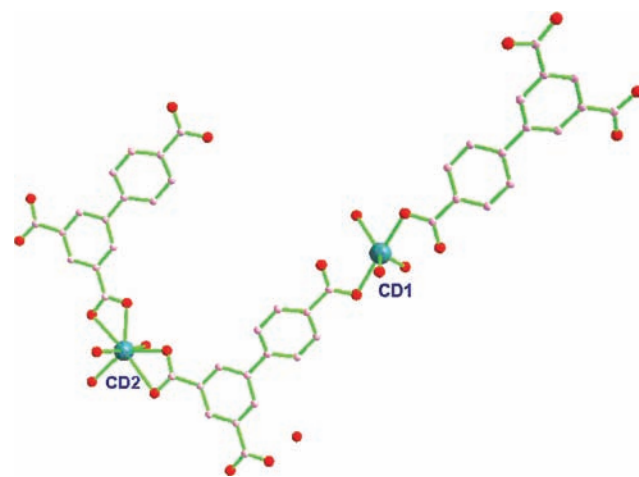


Figure 1. Coordination environments of the cadmium(II) ions.

atom is five-coordinated by two carboxylate oxygen atoms from two BPT ligands [Cd–O 2.233(3) Å] and three oxygen atoms of three coordinated water molecules [Cd–O 2.271(7) and 2.304(5) Å] to generate a trigonal-bipyramidal coordination geometry. Different from Cd(1), the Cd(2) atom has a distorted pentagonal-bipyramidal geometry, with two pairs of chelating carboxylate oxygen atoms provided by two different BPT ligands [Cd–O 2.273(4)–2.564(4) Å] and three coordinated water molecules [Cd–O 2.281(4)–2.322(4) Å]. The cadmium centers are bridged by BPT to form an infinite single-stranded right-handed helix running along the *b* axis (Figure 2a) with a pitch of 7.338(2) Å, which is equal to the length of the crystallographic *b* axis. This steric orientation of the right-handed helix leads to the formation of the wall of a tetragonal nanotube with an opening of 1.0 × 2.5 nm (Cd...Cd; Figure 2b).

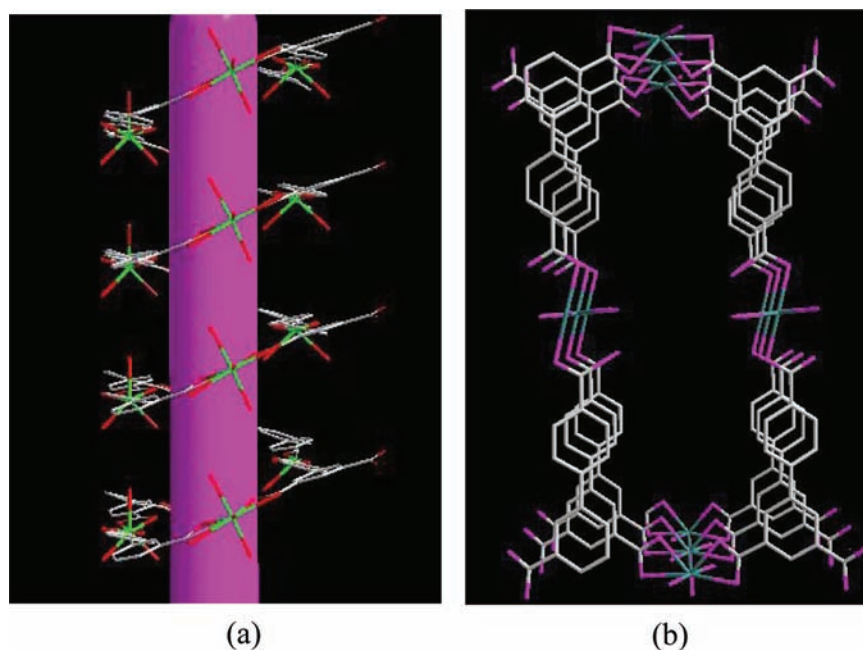


Figure 2. (a) View of the right-handed helical chains. (b) Top view of the single-stranded helical nanotube.

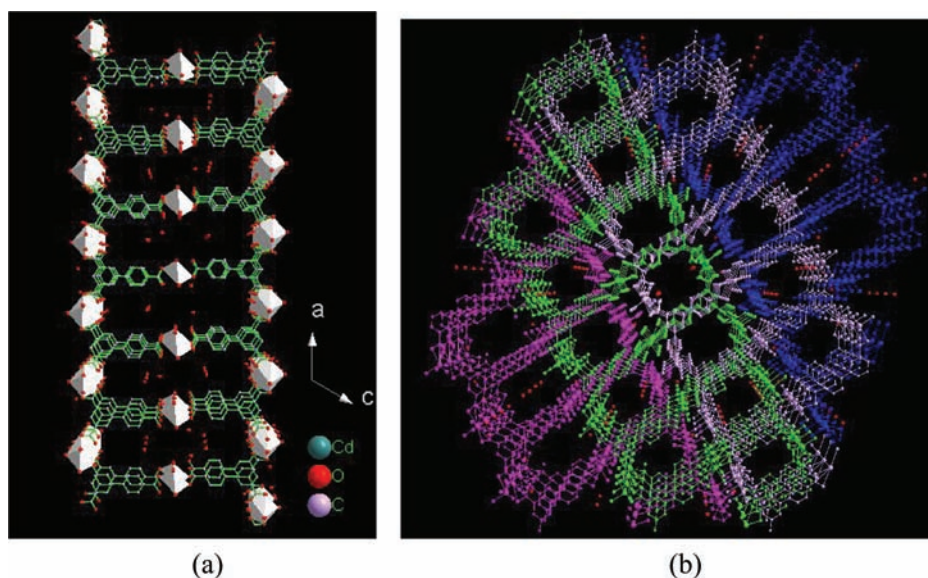


Figure 3. (a) Ladderlike layer constructed via the helical chains. (b) Interdigitated 3D framework viewed in the *b* direction.

The most fascinating structural feature of Cd-1 is that each helical nanotube is not chemistry-independent. As mentioned above, the BPT ligand has three flexible carboxylic binding sites, so the helical nanotubes of Cd-1 extend upward and downward to coordinate the cadmium(II) ions of neighboring helical nanotubes to give rise to a 2D ladderlike layer framework along the *a* axis. As illustrated in Figure 3a, all of the Cd(II) atoms with trigonal-bipyramidal coordination geometry are in the “middle rails” of the ladders, and the width of the ladders is 25.07(113) Å ($\text{Cd}_2 \cdots \text{Cd}_2$). It is a common phenomenon for frameworks with relatively large voids to interdigitate each other to make a more stable architecture. So, the ladder layers of Cd-1 are further interdigitated to generate a 3D polar framework, and two types of channels are formed in the 3D network along the *b* axis with guest water molecules occupied. One is the overlap space between neighboring chiral nanotubes

with dimensions of 10.26×10.33 Å, and the other is the small hollow tube with a size of 10.26×2.51 Å (Figure 3b). Representations of the beautiful topologies are presented in Figure S1 in the Supporting Information. The notability of Cd-1 is that all helical chains in the layer show the same chirality, and the adjacent ladderlike layers also display identical chirality, so this gives rise to a 3D interdigitated chiral porous framework, which combines the features of nanotubes, porosity, and chirality. Calculations using PLATON¹⁹ based on the crystal structure show that the total solvent-accessible volume is 667.2 Å³ per unit cell, comprising 33.1% of the total crystal volume.

Thermal Studies. TGA of Cd-1 shows a weight loss of 18.62% from 25 to 160 °C, which is attributed to the loss of both the guest and coordinated water molecules (expected 17.99%). Also, the host framework is stable up to ca. 360 °C (Figure S2 in the Supporting Information). PXRD character-

ization discovered that it became amorphous after activation at 160 °C, and, interestingly, after immersion in water at room temperature for a few hours, the activated samples resumed their original crystalline forms, which were monitored by PXRD analyses (Figure 4). The reversible transformation suggests that

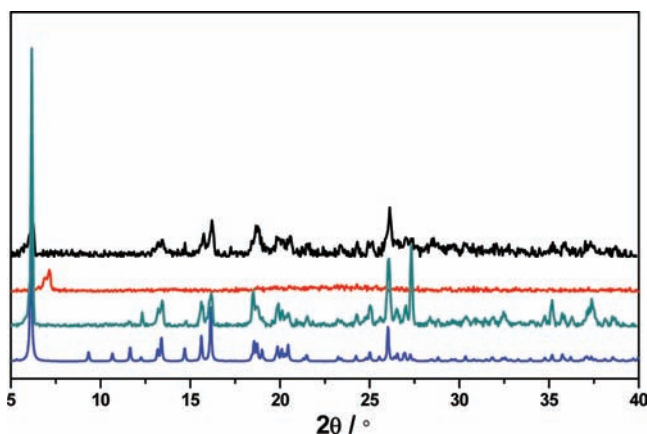


Figure 4. PXRD patterns of simulated Cd-1 (blue) and as-synthesized (green), desolvated (red), and water-immersed desolvated (black) samples.

the framework of Cd-1 is flexible and durable, which results from the flexible organic linkers and π - π stacking. The 3D framework has bistable forms and can alter the forms in response to the temperature and external solvent molecules,²⁰ and such a dynamic structural transformation based on the flexible framework is one of the most interesting phenomena for flexible coordination polymers.²¹

Spectroscopic Properties. In the FT-IR spectra of Cd-1, the O-H stretching frequency of the broad band around 3392 cm^{-1} indicates the presence of water molecules in Cd-1, and two peaks that appear at 1615 and 1442 cm^{-1} are expected for absorption of the asymmetric and symmetric stretching vibrations of the carboxylate groups (Figure S3 in the Supporting Information). The UV absorption spectrum of Cd-1 indicates that it is transparent in the visible region with an absorption edge of 342 nm (Figure S4 in the Supporting Information). The optical diffuse-reflectance study reveals an optical band gap of 3.63 eV for Cd-1, making it a wide-band-gap semiconductor (Figure 5).

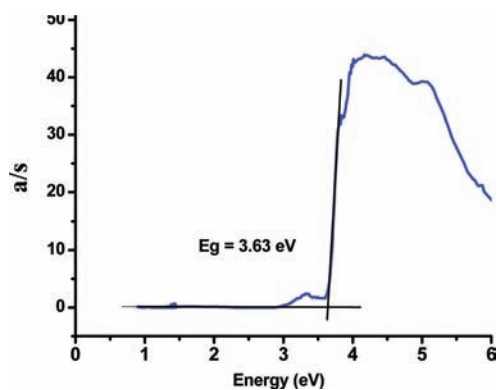


Figure 5. Optical diffuse-reflectance spectrum for Cd-1 with a band gap of 3.63 eV.

We have also examined the photoluminescent properties of Cd-1 in the solid state at room temperature (Figure S5 in the Supporting Information). It exhibits an intense emission of 380 nm upon excitation at 323 nm, which is a blue shift, compared with that of the pure H_3BPT ligand with an emission of 395 nm, which indicates that the emission band of Cd-1 is due to intraligand charge transfer.²²

SHG and Ferroelectric Properties. SHG measurements on powder samples of Cd-1 were carried out to confirm its acentricity as well as to evaluate its potential as a second-order NLO material. The results reveal that Cd-1 displays modest SHG efficiencies, approximately 2.5 times that of potassium dihydrogen phosphate (KDP), indicating the obvious effects of the chirality and helices on the SHG efficiency in Cd-1. Furthermore, the curves of the SHG signal as a function of the particle size from measurements made on powders by the sieving of crystals of Cd-1 into various particle sizes, ranging from 45 to 190 μm , reveal that the material has phase-matching behavior (Figure 6). On the other hand, Cd-1 is air-stable and

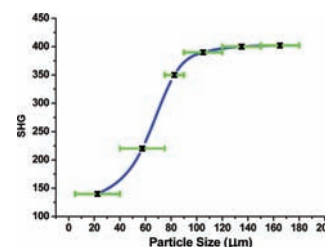


Figure 6. Phase-matching curve for Cd-1.

insoluble in water and common organic solvents, so it is potentially a good candidate for second-order NLO materials. Because Cd-1 crystallizes in the space group C_2 , belonging to 1 of the 10 polar point groups (C_1 , C_2 , C_2v , C_4 , C_4v , C_3 , C_3v , C_6 , and C_6v), required for the ferroelectric properties, its ferroelectric properties were also examined. The hysteresis loop of the electric polarization was obtained for Cd-1, as shown in Figure S6 in the Supporting Information. At room temperature, the remanent polarization (P_r) is ca. 25 nC cm^{-2} with a coercive field (E_c) of ca. 10.48 kV cm^{-1} . The saturation spontaneous polarization (P_s) is ca. 39 nC cm^{-2} , which is smaller than that of the typical ferroelectric KDP (P_s : 5.0 $\mu\text{C cm}^{-2}$).

CONCLUSION

In summary, we have successfully synthesized a chiral coordination nanotube (Cd-1) based on right-handed helical chains from achiral components. The flexible chiral nanotubular framework results in dynamic structural transformation and polarity for Cd-1, which exhibits intriguing ferroelectric and NLO properties with phase-matching behavior. Further efforts will focus on the construction of novel chiral coordination polymers with potential ferroelectric and NLO properties.

ASSOCIATED CONTENT

Supporting Information

X-ray crystallographic data in CIF format, structures, hysteresis loop, photoluminescent spectra, TGA, IR, and PXRD patterns. This material is available free of charge via the Internet at <http://pubs.acs.org>.

AUTHOR INFORMATION

Corresponding Author

*E-mail: jhluo@fjirsm.ac.cn.

ACKNOWLEDGMENTS

This work was financially supported by the National Nature Science Foundation of China (Grants 21171166 and 51102231), the 973 Key Programs of the MOST (Grants 2010CB933501 and 2011CB935904), and the One Hundred Talent Program of the Chinese Academy of Sciences.

REFERENCES

- (1) (a) Cao, X. Y.; Zhang, J.; Cheng, J. K.; Kang, Y.; Yao, Y. G. *CrystEngComm* **2004**, *6*, 315. (b) Dai, F. N.; He, H. Y.; Sun, D. F. *J. Am. Chem. Soc.* **2008**, *130*, 14064.
- (2) (a) Hong, M. C.; Zhao, Y. J.; Su, W. P.; Cao, R.; Fujita, M.; Zhou, Z. Y. *Angew. Chem., Int. Ed.* **2000**, *39*, 2468. (b) Fenniri, H.; Mathivanan, P.; Vidale, K. L.; Sherman, D. M.; Hallenga, K.; Wood, K. V.; Stowell, J. G. *J. Am. Chem. Soc.* **2001**, *123*, 3854. (c) Yaghi, O. M.; O'Keeffe, M.; Ockwig, N. W.; Chae, H. K.; Eddaoudi, M.; Kim, J. *Nature* **2003**, *423*, 705–714. (d) Lu, Z. Z.; Zhang, R.; Li, Y. Z.; Guo, Z. J.; Zheng, H. G. *J. Am. Chem. Soc.* **2010**, *133*, 4172. (e) Ma, S. Q.; Simmons, J. M.; Yuan, D. Q.; Li, J. R.; Weng, W.; Liu, D. J.; Zhou, H. C. *Chem. Commun.* **2009**, 4049. (f) Luo, T. T.; Wu, H. C.; Jao, Y. C.; Huang, S. M.; Tseng, T. W.; Wen, Y. W.; Lee, G. H.; Peng, S. M.; Lu, K. L. *Angew. Chem.* **2009**, *121*, 9625.
- (3) (a) Wang, X. L.; Qin, C.; Wang, E. B.; Xu, L.; Su, Z. M.; Hu, C. W. *Angew. Chem., Int. Ed.* **2004**, *43*, 5036. (b) Su, C. Y.; Goforth, A. M.; Smith, M. D.; Pellechia, P. J.; Zur Loye, H. C. *J. Am. Chem. Soc.* **2004**, *126*, 3576.
- (4) (a) *Chirality in Industry II* Collins, A. N., Sheldrake, G. N., Crosby, J., Eds.; Wiley: New York, 1998. (b) Lin, W. B. *MRS Bull.* **2007**, *32*, 544.
- (5) (a) Cui, Y.; Lee, S. J.; Lin, W. B. *J. Am. Chem. Soc.* **2003**, *125*, 6014. (b) Wu, C. D.; Hu, A.; Zhang, L.; Lin, W. B. *J. Am. Chem. Soc.* **2005**, *127*, 8940. (c) Jiang, H. W. B. *J. Am. Chem. Soc.* **2006**, *128*, 11286.
- (6) Huang, Y. G.; Mu, B.; Schoenecker, P. M.; Carson, C. G.; Karra, J. K.; Cai, Y.; Walton, K. S. *Angew. Chem., Int. Ed.* **2010**, *49*, 1–6.
- (7) (a) Li, G.; Yu, B.; Cui, Y. *J. Am. Chem. Soc.* **2008**, *130*, 4582. (b) Yuan, G. Z.; Zhu, C. F.; Liu, Y.; Xuan, W. M.; Cui, Y. *J. Am. Chem. Soc.* **2009**, *131*, 10452.
- (8) Train, C.; Nuida, T.; Gheorghe, R.; Gruselle, M.; Ohkoshi, S. I. *J. Am. Chem. Soc.* **2009**, *131*, 16838.
- (9) Hang, T.; Zhang, W.; Ye, H. Y.; Xiong, R. G. *Chem. Soc. Rev.* **2011**, *40*, 3577.
- (10) (a) Lee, H. N.; Hesse, D.; Zakharov, N.; Gosele, U. *Science* **2002**, *296*, 2006. (b) Naumov, I. I.; Bellaiche, L.; Fu, H. *Nature* **2004**, *432*, 737. (c) Ahn, C. H.; Rabe, K. M.; Triscone, J. M. *Science* **2004**, *303*, 488.
- (11) (a) Lee, H. N.; Christen, H. M.; Chisholm, M. F.; Rouleau, C. M.; Lowndes, D. H. *Nature* **2005**, *433*, 395. (b) Rijnders, G.; Blank, D. H. V. *Nature* **2005**, *433*, 369.
- (12) (a) Gu, Z. G.; Zhou, X. H.; Jin, Y. B.; Xiong, R. G.; Zuo, J. L.; You, X. Z. *Inorg. Chem.* **2009**, *48*, 8069. (b) Xu, G. C.; Zhang, W.; Ma, X. M.; Chen, Y. Y.; Zhang, L.; Cai, H. L.; Wang, Z. M.; Xiong, R. G.; Gao, S. J. *J. Am. Chem. Soc.* **2011**, *133*, 14948. (c) Xu, G.; Zhou, W. W.; Wang, G. J.; Long, X. F.; Cai, L. Z.; Wang, M. S.; Guo, G. C.; Huang, J. S.; Bater, G.; Jakubas, R. *J. Mater. Chem.* **2009**, *19*, 2179. (d) Zhang, W.; Cai, H. L.; Ge, J. Z.; Xiong, R. G.; Huang, S. P. D. *J. Am. Chem. Soc.* **2010**, *132*, 7300. (e) Ye, Q.; Wang, X. S.; Zhao, H.; Xiong, R. G. *Chem. Soc. Rev.* **2005**, *34*, 208. (f) Cai, H. L.; Zhang, W.; Ge, J. Z.; Zhang, Y.; Awaga, K.; Nakamura, T.; Xiong, R. G. *Phys. Rev. Lett.* **2011**, *107*, 147601.
- (13) (a) Liu, Q. Y.; Wang, Y. L.; Shan, Z. M.; Cao, R.; Jiang, Y. L.; Wang, Z. J.; Yang, E. L. *Inorg. Chem.* **2010**, *49*, 8191. (b) Wang, S. N.; Xing, H.; Li, Y. Z.; Bai, J. F.; Scheer, M.; Pan, Y.; You, X. Z. *Chem. Commun.* **2007**, 2293. (c) Guo, Z. G.; Cao, R.; Wang, X.; Li, H. F.; Yuan, W. B.; Wang, G. J.; Wu, H. H.; Li, J. *J. Am. Chem. Soc.* **2009**, *131*, 6894. (d) Chen, P.; Nan, J. P.; Dong, X. L.; Ren, X. M.; Jin, W. Q. *J. Am. Chem. Soc.* **2011**, *133*, 12330. (e) Lin, W. B.; Wang, Z. Y.; Ma, L. J. *J. Am. Chem. Soc.* **1999**, *121*, 11249. (f) Qu, Z. P.; Zhao, H.; Wang, X. S.; Li, Y. H.; Song, Y. M.; Liu, Y. J.; Ye, Q.; Xiong, R. G.; Abrahams, B. F.; Xue, Z. L.; You, X. Z. *Inorg. Chem.* **2003**, *42*, 7710. (g) Wang, C.; Zhang, T.; Lin, W. *Chem. Rev. Articles ASAP*. (h) Liu, Y.; Li, G.; Li, X.; Cui, Y. *Angew. Chem., Int. Ed.* **2007**, *46*, 6301. (i) Xiong, R. G.; X, X.; Zhao, H.; You, X. Z.; Abrahams, B. F.; Xue, Z. L. *Angew. Chem., Int. Ed.* **2002**, *41*, 3800.
- (14) (a) Wong-Foy, A. G.; Lebel, O.; Matzger, A. J. *J. Am. Chem. Soc.* **2007**, *129*, 15740. (b) Schnobrich, J. K.; Cychosz, K. A.; Dailly, A.; Wong-Foy, A. G.; Lebel, O.; Matzger, A. J. *J. Am. Chem. Soc.* **2010**, *133*, 13941. (c) Guo, Z. R.; Li, G. H.; Zhou, L.; Su, S. Q.; Lei, Y. Q.; Dang, S.; Zhang, H. J. *Inorg. Chem.* **2009**, *48*, 8069.
- (15) Kubelka, P.; Munk, F. Z. *Tech. Phys.* **1931**, *12*, 593.
- (16) Kurtz, S. W.; Perry, T. T. *J. Appl. Phys.* **1968**, *39*, 3798.
- (17) *CrystalClear*, version 1.36; Molecular Structure Corp. and Rigaku Corp.: The Woodlands, TX, and Tokyo, Japan, 2000.
- (18) Sheldrick, G. M. *SHELXS 97, Program for Crystal Structure Solution*; University of Göttingen: Göttingen, Germany, 1997.
- (19) Spek, A. L. *PLATON, A Multipurpose Crystallographic Tool*; Utrecht University: Utrecht, The Netherlands, 1999.
- (20) Kitagawa, S.; Knodo, M. *Bull. Chem. Rev. Jpn.* **1998**, 711739.
- (21) (a) Kitagawa, S.; Kitaura, R.; Noro, S. *Angew. Chem., Int. Ed.* **2004**, *43*, 2334. (b) Noro, S.; Kitaura, R.; Knodo, M.; Kitagawa, S.; Ishii, T.; Matsuzaka, H.; Yamashita, M. *J. Am. Chem. Soc.* **2002**, *124*, 2568. (c) Zhang, J. P.; Lin, Y. Y.; Zhang, W. X.; Chen, X. M. *J. Am. Chem. Soc.* **2005**, *127*, 14162. (d) Hu, S.; Zhang, J. P.; Tong, M. L.; Chen, X. M.; Kitagawa, S. *Cryst. Growth Des.* **2007**, *7*, 2286.
- (22) (a) Huang, Y. Q.; Ding, B.; Song, H. B.; Zhao, B.; Ren, P.; Cheng, P.; Wang, H. G.; Liao, D. Z.; Yan, S. P. *Chem. Commun.* **2006**, 4906. (b) Huang, K. L.; Liu, X.; Chen, X.; Wang, D. Q. *Cryst. Growth Des.* **2009**, *9*, 1646. (c) Zhao, H.; Qu, Z. R.; Ye, H. Y.; Xiong, R. G. *Chem. Soc. Rev.* **2008**, *37*, 84.